OPEN

Investigation of Fluorodeoxyglucose Positron Emission Tomography for the Diagnosis of Solid Pseudopapillary Neoplasm of the Pancreas

A Study Associated With a National Survey of Solid Pseudopapillary Neoplasms

Keisuke Kurihara, MD, Keiji Hanada, MD, PhD,† Masahiro Serikawa, MD, PhD,* Yasutaka Ishii, MD, PhD,* Tomofumi Tsuboi, MD, PhD,* Ryota Kawamura, MD,* Tsuyoshi Sekitou, MD,* Shinya Nakamura, MD,* Takeshi Mori, MD,* Tetsuro Hirano, MD,* Juri Ikemoto, MD,* and Kazuaki Chayama, MD, PhD**

Objectives: This study aimed to investigate the utility of fluorodeoxyglucose (FDG) positron emission tomography for solid pseudopapillary neoplasm (SPN) diagnosis.

Methods: The subjects included 53 cases of SPN. We compared the maximal standardized uptake volume (SUVmax) with those of 25 cases of pancreatic duct cancer and 18 cases of pancreatic neuroendocrine neoplasm. In addition, immunopathological testing for SPN with regard to FDG uptake was undertaken.

Results: An increase in SUVmax was observed in all tumors with increased tumor diameter. Among tumors of 20 mm or smaller, the SUVmax of SPN was significantly higher than those of pancreatic duct cancer and pancreatic neuroendocrine neoplasm. The results of a pathological study of FDG uptake in SPN revealed increased glucose transporter protein type 1 expression with tumor enlargement. Furthermore, increased hypoxia-inducible factor-1 and vascular endothelial growth factor expression under hypoxic conditions were observed in the areas of necrosis.

Conclusions: In cases in which high FDG uptake is observed in small pancreatic tumors, FDG positron emission tomography is potentially useful for SPN differentiation. The factors involved in FDG uptake in SPN include cell density and glucose transporter protein expression, as well as hypoxia-inducible factor and vascular endothelia growth factor expression in the hypoxic environment of necrotic areas.

Key Words: solid pseudopapillary neoplasm, FDG-PET, pancreas, pancreatic duct cancer, pancreatic neuroendocrine neoplasm, tumor

Abbreviations:
FDG-PET - fluorodeoxyglucose positron emission tomography,
SPN - solid pseudopapillary neoplasm,
SUVmax - maximal standardized uptake volume,
PDC - pancreatic duct cancer,
PNEN - pancreatic neuroendocrine neoplasm,
GLUT1 - glucose transporter protein type 1,
HIF - hypoxia-inducible factor, VEGF - vascular endothelial growth factor,
JPS - Japan Pancreas Society, CT - contrast computed tomography

(*Pancreas* 2019;48: 1312–1320)

Solid pseudopapillary neoplasm (SPN) in the pancreas is a relatively rare pancreatic epithelial tumor that often occurs in young women and is reported to occur in 0.17% to 2.7% of all pancreatic tumors.[1] With advances in imaging examinations, reports of SPN have increased in recent years.[2–5] We conducted our own investigation using data from the Japan Pancreas Society (JPS) SPN National Survey to study the clinical pathology of this disease. The results of the National Survey revealed that the typical macroscopic findings of SPN included a mixture of cysts and solid components, calcification, and bleeding. Contrast computed tomography (CT) examinations revealed prolonged, uneven staining, with tumors depicted with cysts and calcification. However, in small SPNs, the tumors may not have cysts, calcification, or bleeding. Therefore, it is often difficult to differentiate SPN from pancreatic duct cancer (PDC).[2]

Fluorodeoxyglucose positron emission tomography (FDG-PET) is useful for the differential diagnosis of malignancies or otherwise of tumorous lesions in various organs. In pancreatic tumors, high FDG uptake is observed in PDC; thus, it has been reported as a marker of malignancy.[6] Furthermore, although World Health Organization classifications consider SPN to have low malignant potential, there are many reports of high FDG uptake.[7–13] The degree of FDG uptake by tumors generally depends on the tumor size, histologic type, and microvessel density at the molecular level,[6] and associations have been reported with glucose transporter-1 (GLUT-1) related to glucose metabolism,[13–15] hypoxia-inducible factor-1 (HIF-1) related to hypoxic environments, and vascular endothelial growth factor (VEGF) related to neovascularization.[16–20]

A National Survey of SPN of the pancreas was conducted by the JPS; we additionally conducted a study to clarify the utility of FDG-PET for the diagnosis of SPN, as well as an investigation of the molecular mechanisms related to FDG uptake.

Committee

The JPS established a committee (Drs Keiji Hanada, Keisueke Kurihara, Takao Itoi, Akio Katanuma, Tamito Sasaki, and Kazuo Hara as endoscopists; Drs Masafumi Nakamura, Wataru Kimura

From the *Department of Gastroenterology and Metabolism, Applied Life Sciences, Institute of Biomedical and Health Sciences, Hiroshima University; and †Department of Gastroenterology, Onomichi General Hospital, Hiroshima, Japan.
Received for publication March 11, 2019; accepted September 12, 2019.
Address correspondence to: Keisuke Kurihara, MD, Department of Gastroenterology and Metabolism, Applied Life Sciences, Institute of Biomedical and Health Sciences, Hiroshima University, 1-2-3 Kasumi, Hiroshima 734-8551, Japan (e-mail: k.kurihara@onomichi-gh.jp).
This study was supported by Japan Pancreas Society. The design and conduct of the study, interpretation of the data, and decision to submit the manuscript for publication were the responsibilities of the authors listed.
This study was approved by the ethics committees of Hiroshima University (E-817).
The authors declare no conflict of interest.

DOI: 10.1097/MPA.0000000000001424

Yutaka Suzuki, and Masanori Sugiyama as surgeons; Drs Nobuyuki Ohike, Noriyoshi Fukushima, and Michio Shimizu as pathologists; and Drs Kousei Ishigami and Toshifumi Gabata as radiologists) to evaluate the clinical and pathological problems associated with SPNs.

MATERIALS AND METHODS

National Survey of SPN of the Pancreas by the JPS

The study subjects included 288 cases that were diagnosed with SPN using postoperative specimens at 33 facilities with councilors on the Board of the JPS, along with a questionnaire-based survey related to the clinical findings. The maximal standardized uptake volume (SUVmax) of the tumor was measured in 53 cases in which FDG-PET was performed and a study was carried out on the utility of FDG-PET in SPN diagnosis and its relationship to the clinical findings. We then compared the FDG uptake in 25 cases of PDC and 18 cases of pancreatic neuroendocrine neoplasm (PNEN) in which surgery had been conducted at our hospital and PET had been performed before surgery.[2]

FDG-PET Contrast Method

The ^{18}F-FDG PET scans were performed on a Biograph mCT-S PET/CT scanner (Siemens, Milwaukee, Wis). The patients fasted for at least 5 hours before the injection of ^{18}F-FDG. Data acquisition was started approximately 60 minutes after the injection of 71 to 333 MBq (range, 1.40–3.67 MBq/kg) of FDG. The imaging range was from the thigh to the head with both arms raised; the imaging length fell within the range of 8 bed positions. The emission acquisition time was 2 minutes in list mode per bed position. The PET images were reconstructed using a 3-dimensional ordered subsets expectation maximization algorithm in a 128 × 128 matrix with a field of view of 200 × 200 mm and a slice thickness of 3 mm.

Immunostaining

To study the molecular mechanisms relating to FDG uptake in SPN, we conducted GLUT-1, VEGF, HIF-1, and CD31 immunostaining using the paraffin-embedded section protocol for 6 cases of SPN in which surgery had been conducted at our hospital and investigated the relationship of the findings with the SUVmax.

Immunostaining was performed using a polymer method and ImmPRESS reagent (Vector Laboratories, Burlingame, Calif). After deparaffinization and hydration, the macrophage method using a citrate buffer Target Retrieval Solution (Dako, Carpinteria, Calif) was used, which included heat treatment for 10 minutes before antigen retrieval. Endogenous enzyme blocking was conducted for 30 minutes with a 0.3% hydrogen peroxide/methanol solution, followed by blocking with 2.5% normal horse serum. The primary antibodies used were as follows: GLUT1 (1:300 dilution, ab652; Abcam, Cambridge, United Kingdom), VEGF-A (1:200 dilution, ab46154; Abcam), HIF-1 (1:500 dilution, ab85886; Abcam), Ki67 (1:50 dilution, ab8191; Abcam), and CD31 (1:300 dilution, bs0195R; Bioss, Woburn, Mass). The antibodies were all left overnight for a response, followed by the use of the ImmPRESS reagent for the secondary antibody reaction. Staining was conducted with the ImmPACT DAB enzyme substrate solution.

Immunostaining was evaluated on the basis of staining concentration and the ratio of tissue stained. The degrees of staining of the GLUT-1, VEGF, and HIF-1 of the cytoplasm and cell membranes were classified into 4 levels: negative (−) or positive (+, ++, or +++). In addition, the number of capillary vessels stained with CD31 was measured in 4 random sites with high vessel density in a visual field of 1:200 (0.8 mm^2) for each sample to measure the microvessel density based on the average value.

Statistical Analysis

We performed statistical analysis using JMP Ver.12.0.1 (SAS Institute Inc, Cary, NC) software program. The Kaplan-Meier method was used to estimate the cumulative survival, and log-rank test was used for between-group comparisons. With respect to 2-tailed tests, the Pearson χ^2 was used to determine statistical significance. The data are presented as mean (standard deviation [SD]), unless stated otherwise.

RESULTS

Patient Characteristics

The National Survey included 53 SPN patients who had undergone FDG-PET imaging (Table 1). The male-to-female ratio was 22:31. The average (SD) age was 37.5 (12.4) years (range, 11–68 years). The sites included the pancreatic head in 15 cases, the pancreatic body in 25 cases, and the pancreatic tail in 13 cases. The average (SD) tumor diameter was 38.4 (28.2) mm (range, 10–130 mm). Computed tomography examinations revealed prolonged staining in 35 cases (66%), calcification in 32 cases (60%), and cysts in 22 cases (42%). Fifteen cases had tumor diameters of 20 mm or smaller, and in 9 of those cases, neither cysts nor calcification was observed; therefore, it was difficult to differentiate between PDC and PNEN by imaging examination. Endoscopic ultrasound-fine needle aspiration was conducted before surgery in 26; 22 of which were diagnosed with SPN. One case was a pancreatic neuroendocrine tumor, and 3 cases were difficult to diagnose because of a low tissue volume. In all cases, preoperative FDG-PET was conducted. Examination of postoperative tissue samples of all cases revealed pseudopapillary structure (characteristic of SPN) and positive β-catenin in immunostaining; thus, the cases were diagnosed as having SPN. In postoperative pathology, extrapancreatic infiltration and lymph node metastases were not observed, but there were 2 cases of lymphatic vessel invasion, 4 cases of vessel invasion, and 8 cases of infiltration into the surrounding nerve plexuses. The average diameter of tumors with vessel invasion or infiltration of the nerve plexuses was 51 mm (30–130 mm); thus, large, and no vessel invasion or nerve plexus infiltration was observed in tumors 20 mm or smaller. Among the 25 patients with PDC, the male-to-female ratio was 14:11, and the average (SD) age was 64.2 (7.8) years (range, 49–76 years), which therefore were significantly higher ($P < 0.001$) compared with SPN. The sites included the pancreatic head in 15 cases, the

TABLE 1. Characteristics of Patients

	SPN	PDC	PNEN
No. patients, n	53	25	18
Sex, male:female, n	22:31	14:11	7:11
Age, mean, y	37.5	64.2	56.9
Location, n			
Head	15	15	7
Body	25	4	4
Tail	13	6	7
Size, mean, mm	38.4	30.2	24.2

Date were expressed as n unless otherwise indicated.

TABLE 2. Comparison of SUVmax Between SPN, PDC, and PNEN

	SPN	PDC	*P*	PNEN	*P*
No. patients, n	53	20		18	
SUVmax, mean	4.9	6.0	0.04	4.4	0.43
SUVmax for each tumor diameter, mm					
≤20	3.9	2.4	0.02	2.6	0.02
21–30	4.6	6.5		4.2	
≥40	5.6	8.7		9.4	

pancreatic body in 4 cases, and the pancreatic tail in 6 cases. The average (SD) tumor diameter was 30.2 (16.2) mm (range, 1–65 mm), and there were 8 cases with tumors of 20 mm or smaller. Finally, in PNEN, the male-to-female ratio was 7:11 in 18 patients, and the average (SD) age was 56.9 (12.5) years (range, 23–73 years). The sites included the pancreatic head in 7 cases, the pancreatic body in 4 cases, and the pancreatic tail in 7 cases. The average (SD) tumor diameter was 24.2 (15.1) mm (range, 6–60 mm), and there were 10 cases with tumors of 20 mm or smaller. In all cases, preoperative PET-CT was performed. There were no distant metastases or infiltration into the surrounding vessels, and the patients were considered suitable for surgery.

Comparative Study of SUVmax in SPN, PDC, and PNEN

The median and average (SD) SUVmax values in SPN were 4.4 (range, 1.8–9.8) and 4.9 (2.6), respectively (Table 2). Based on the normal SUVmax cutoff value of 3 for positivity, the FDG-PET positivity rate was 77% (41 cases). Nine of 15 cases with tumors of 20 mm or smaller were FDG-PET positive. The average tumor diameter in the positive cases was 41 mm, which was significantly larger than the 22 mm in the negative cases ($P = 0.016$). A positive correlation was observed in terms of the relationship between SPN tumor diameter and SUVmax (Fig. 1, correlation coefficient (r) = 0.45, P = 0.007). The average SUVmax values were 3.9 for tumor diameters up to 20 mm, 4.6 for those measuring 21 to 30 mm, and 5.6 for those measuring 41 to 50 mm; therefore, SUVmax increased with tumor diameter. Furthermore, the average SUVmax value in the 9 cases with vessel invasion or nerve plexus infiltration was 6.2, which was significantly higher than the average value of 4.6 for cases without vessel invasion or nerve plexus infiltration ($P = 0.04$).

The median and mean (SD) SUVmax values for PDC were 6.5 (range, 2.1–10) and 6.1 (2.8), respectively, which were significantly higher than the values for SPN ($P = 0.04$). If the SUVmax cutoff value was set to 3, there were 18 cases with PET positivity (72%). In tumors with a diameter of 20 mm or smaller, only 1 of 8 cases was FDG-PET positive. A positive correlation was observed between tumor diameter and SUVmax (Fig. 1, correlation coefficient (r) = 0.76, $P = 0.005$). The average SUVmax values were 2.5 for tumor diameter up to 20 mm, 6.5 for tumor diameters of 21 to 30 mm, and 8.7 for tumor diameters of 41 to 50 mm.

The median and average (SD) SUVmax values for PNEN were 3.3 (range, 1.2–20.7) and 4.4 (4.3), respectively, which did not differ significantly from those for SPN. If the SUVmax cutoff value was set to 3, 11 cases were PET positive (61%). In tumors of 20 mm or smaller, only 3 of 10 cases were FDG-PET positive. A positive correlation was observed between tumor diameter and SUVmax (Fig. 1, correlation coefficient (r) = 0.78, P = 0.003). The average SUVmax values were 2.6 for tumor diameters up to 20 mm, 4.2 for tumor diameters of 21 to 30 mm, and 9.4 for tumor diameters of 41 to 50 mm.

Therefore, in SPN, PDC, and PNEN, an enlargement of tumor diameter led to increased SUVmax. In addition, the average

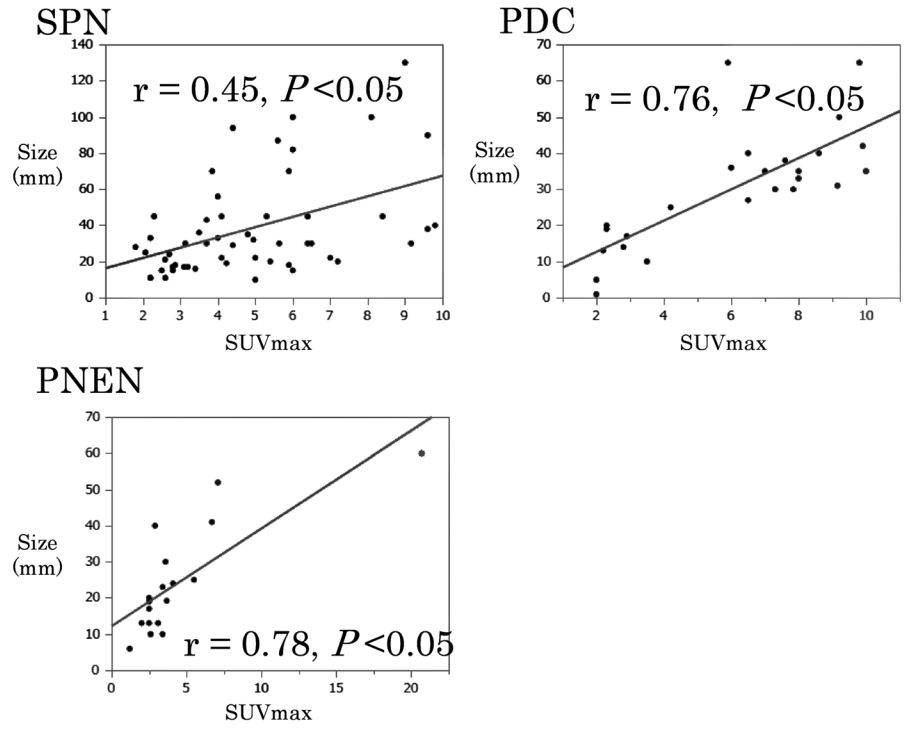

FIGURE 1. A positive correlation was observed between tumor diameter and SUVmax for SPN, PDC, and PNEN.

TABLE 3. Histopathological Characteristics and Immunohistological Evaluations

						GLUT*		VEGF*		HIF-1*		
No.	Size, mm	SUVmax	Necrosis	Cyst	Bleeding	Solid	Necrosis	Solid	Necrosis	Solid	Necrosis	MVD/0.8 mm^2
1	11	2.2	+	−	−	−	++	−	+	−	+	42
2	15	3.1	+	−	−	+	++	−	+	−	+	40
3	18	3.4	++	+	++	+	++	+	+	+	+	44
4	22	6	+	−	+	++	+++	+	++	+	++	48
5	23	5.6	+++	−	+	+	+++	+	+++	+	++	55
6	30	4.8	+++	++	++	++	+++	+	+++	+	+++	56

*Immunohistochemical staining was evaluated for solid place and necrosis place in the tumor.

+++, strongly positive; ++, mildly positive; +, weakly positive; −, negative; MVD, microvessel density.

SUVmax value was significantly higher in PDC than that for SPN ($P = 0.04$), and no significant difference was observed between PNEN and SPN. However, the average SUVmax in tumors 20 mm or smaller was significantly higher for SPN than those for PDC and PNEN (SPN vs PDC: 3.9 vs 2.5, $P = 0.02$; SPN vs PNEN: 3.9 vs 2.6, $P = 0.02$). There were few cases of FDG-PET positivity among PDC cases with tumors measuring 20 mm or smaller (1/8 cases) and only 3 of 10 PNEN cases. Nine of 15 SPN tumors measuring 20 mm had PET positivity. Therefore, compared with that in PDC and PNEN, high FDG uptake was observed in SPN while the tumor diameter was small.

Histopathological Characteristics and Immunohistological Evaluations

To investigate the factors relating to FDG uptake in SPN, an evaluation of the histopathological characteristics and GLUT1, VEGF, HIF-1, and CD31 immunostaining were conducted in 6 cases of SPN in which surgery was performed at this hospital and in which postoperative evaluation using the paraffin-embedded section protocol could be used (Table 3). In terms of patient characteristics, the average (SD) age was 34.2 (14.3) years, the average (SD) tumor diameter was 19.8 (6.7) mm, and the average SUVmax was 4.2 (1.5; Table 4).

The basic pathological findings of SPN indicated that it was a solid tumor with a dense presentation of small, round cells with nuclei, surrounding a pseudopapillary structure. In addition, the internal characteristics differed significantly depending on tumor diameter. In cases 1 and 2, with small tumor diameters, there were no cysts or bleeding, and both had solid tumors with extremely high cell densities (Figs. 2A, B). Both cases had small areas of necrosis in the middle of the tumor, which included a number of instances of small-scale follicular degeneration of the tumor cells (Fig. 2C). Fibrous septal structures were observed, and involvement of the surrounding pancreatic tissue was observed in areas with no septum (Fig. 2D). With an increase in tumor diameter, there was more bleeding and necrosis. In cases 5 and 6, with large tumor diameters, necrotic changes were widespread within the tumor, with widespread findings of bleeding also observed (Figs. 3A, B). Furthermore, a comparison of cases 1 and 2 revealed large-scale follicular degeneration in the intercellular spaces of the area of necrosis, with some cyst formation, and reduced cell density in the areas of necrosis (Fig. 3C).

Immunostaining of GLUT1 revealed heavy staining in the tumor nuclei, whereas staining of the cytoplasm and cellular membrane differed depending on the internal characteristics. In solid areas, there was only weak staining of the cytoplasm and cellular membranes, whereas relatively strong staining was observed in areas of necrosis (Fig. 4). In case 1, with a small tumor diameter, no cytoplasmic staining in the solid area and weak staining in the area of necrosis were observed (Figs. 4A, B). Increased tumor diameter led to staining of the membranous and cytoplasm in the solid area and strong staining in the area of necrosis (Figs. 4C, D). In addition, in masses with a large tumor diameter, the necrosis was widespread, with correspondingly widespread areas of staining. Staining for HIF-1 and VEGF was weak in the solid areas of the tumor, as was observed for GLUT-1, and relatively strong staining was observed in the necrotic area. The level of staining increased with increasing tumor diameter. In case 1, with a small tumor diameter, staining was weak in the area of necrosis; however, in cases 5 and 6, relatively strong staining was observed in solid areas and strong staining was observed in the areas of necrosis (Figs. 5, 6). Microvessel density stained with CD31 revealed an increase corresponding to the increase in tumor diameter; however, the difference was not statistically significant ($P = 0.15$). Furthermore, evaluation of the microvessel characteristics indicated that the individual vessels were very small in the solid area of the tumor, whereas the area of necrosis had thickening of the vascular walls and crossover of vessels. These changes were more often observed in tumors with large diameters (Fig. 7).

DISCUSSION

There remain many unknown factors in the molecular mechanisms and clinical conditions of SPN. Under World Health Organization classification, SPN has low malignant potential, but metastases occur occasionally.[2–5] In a previous National Survey on SPN, we investigated the clinical pathology characteristics of 288 cases. The clinical characteristics included 5 cases (1.7%) with distant metastases, and postoperative recurrence was observed in 6 cases (2.1%); however, the 5-year survival rate was good at 98.8%, and complete resection is reported to be important for treatment. The reported pathological characteristics include a

TABLE 4. Characteristics of SPN Patients

No.	Sex	Age, y	Location	Size, mm	SUVmax
1	Female	36	Body	11	2.2
2	Male	48	Body	15	3.1
3	Male	35	Head	18	3.4
4	Female	21	Head	22	6
5	Male	14	Head	23	5.6
6	Female	50	Tail	30	4.8

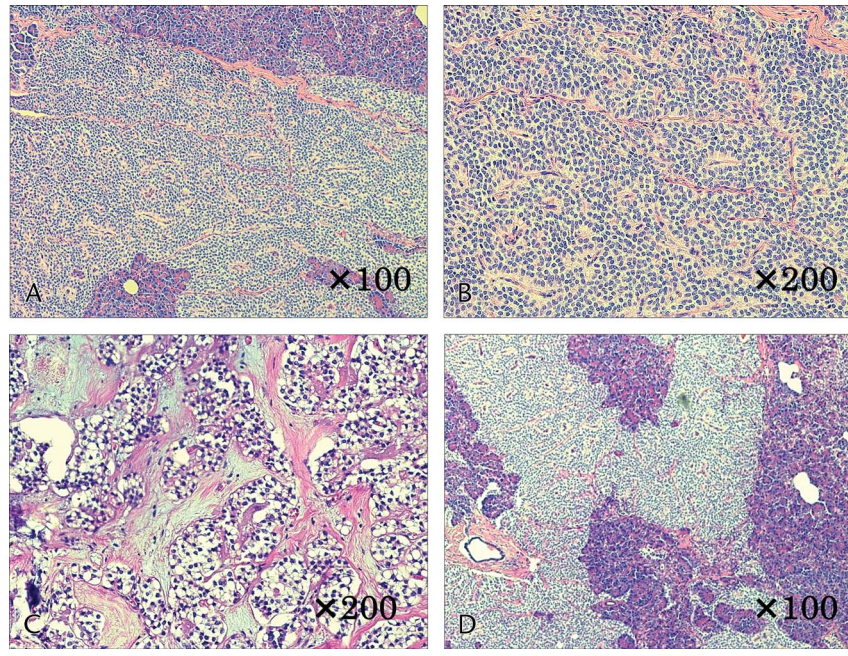

FIGURE 2. Histological findings of case 1. A and B, Monomorphic epithelial cells cohered in high density and forming solid and pseudopapillary structures. C, Small areas of necrosis in the middle of the tumor, which included a number of instances of small-scale follicular degeneration of the tumor cells. D, Involvement of the surrounding pancreatic tissue was observed in areas with no septum.

higher likelihood of degeneration such as cysts or calcification with increasing tumor diameter, whereas small tumors of 2 cm or smaller are often observed as solid tumors without these types of degeneration.[2] Even among the 53 cases in our study, a number had tumors of 2 cm or smaller without cysts or calcification; thus, the differential diagnosis between PDC or PNEN is difficult with imaging examinations alone.

Previous reports on FDG-PET in SPN did not observe a high uptake of FDG[21,22]; however, high intake is reported in most cases.[7–13] Furthermore, a report comparing FDG uptake in SPN, PDC, and PNEN suggested that the lower limit of SUVmax was potentially useful for the differentiation of PDC and PNEN.[9] A report on similarly sized tumors stated that FDG uptake is often observed in SPN compared with that in PDC but is difficult to

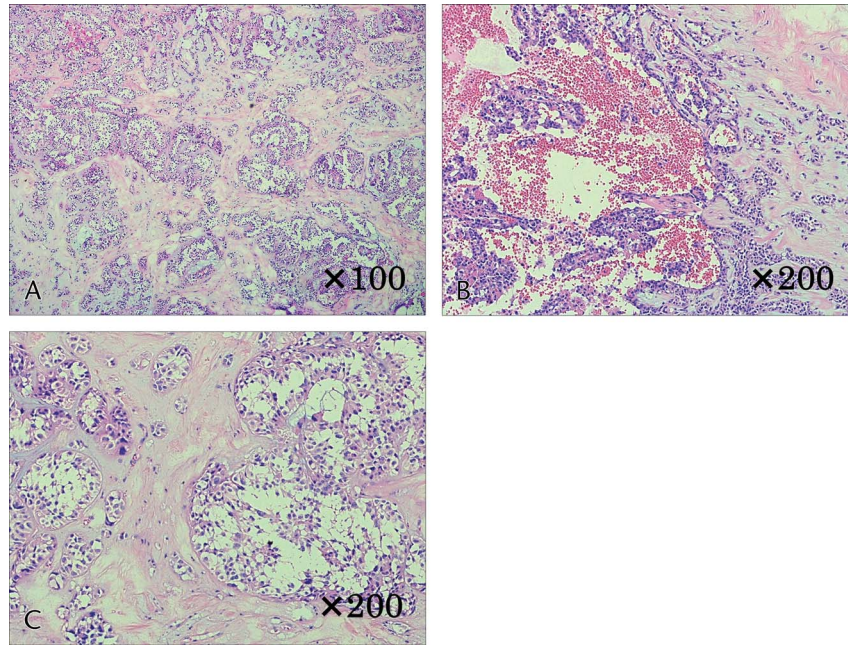

FIGURE 3. Histological findings of case 6. A and B, Necrotic changes were widespread within the tumor, with widespread findings of bleeding also observed. C, Large-scale follicular degeneration in the intercellular spaces of the area of necrosis, with some cyst formation, and reduced cell density in the areas of necrosis.

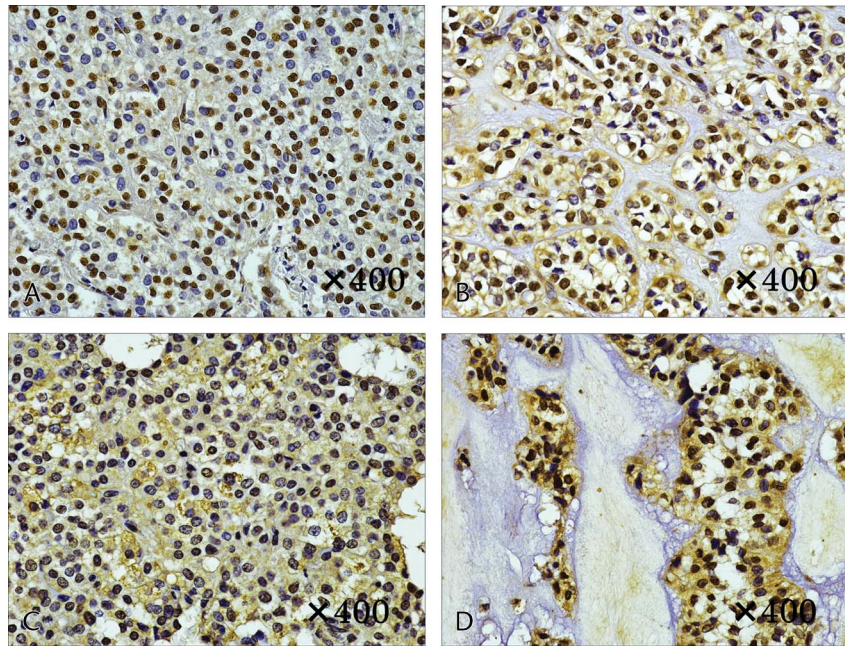

FIGURE 4. Immunostaining of GLUT-1. A and B, Case 1. A, No cytoplasmic staining in the solid area. B, Weak membranous and cytoplasmic staining in the area of necrosis. C and D, Case 6. C, Weak membranous and cytoplasmic staining in the solid area. D, Strong membranous and cytoplasmic staining in the area of necrosis.

differentiate by FDG-PET alone.[11] With regard to the differentiation between malignant and benign SPN, cases with vessel invasion and metastases have significant FDG uptake and there are also reports that FDG-PET is useful for the diagnosis of SPN stage.[10,11]

In our study, the overall comparison of SUVmax between SPN, PDC, and PNEN revealed significantly higher SUVmax of PDC and no significant difference with SPN and PNEN. However, in small tumors of 20 mm or smaller, PET positivity was observed in 9 (60%) of 15 cases in SPN, whereas there were 1 (13%) of 8 cases of PDC and in 3 (30%) of 10 cases of PNEN. The average SUVmax for SPN measuring 20 mm or smaller was 3.9, significantly higher than 2.5 for PDC and 2.6 for PNEN. As with previous reports, it is difficult to differentiate between SPN, PDC, and PNEN using only FDG-PET,[9] but in SPN with small tumor diameter, high FDG uptake is more often observed. In

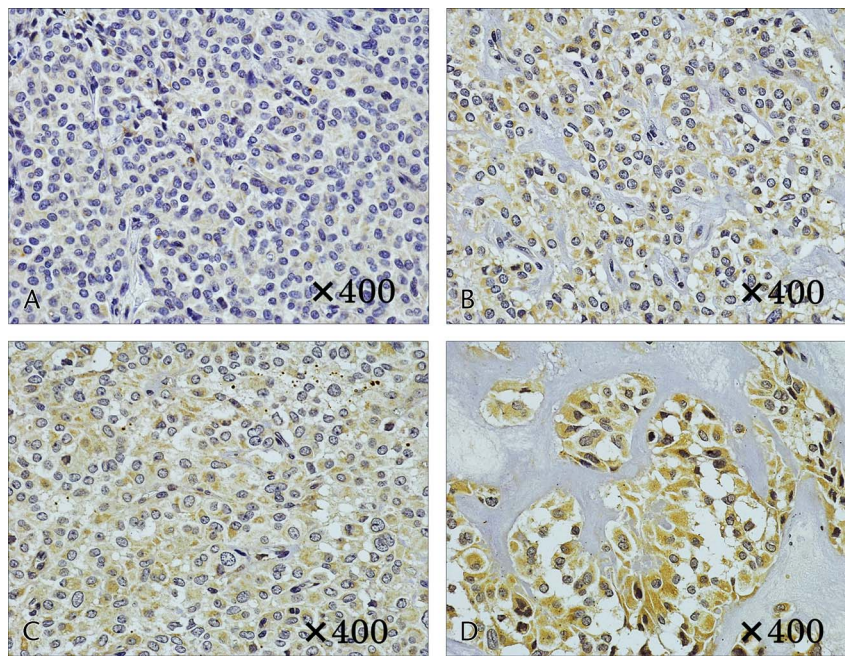

FIGURE 5. Immunostaining of HIF-1. A and B, Case 1. A, No cytoplasmic staining in the solid area. B, Weak cytoplasmic staining in the area of necrosis. C and D, Case 6. C, Weak cytoplasmic staining in the solid area. D, Strong cytoplasmic staining in the area of necrosis.

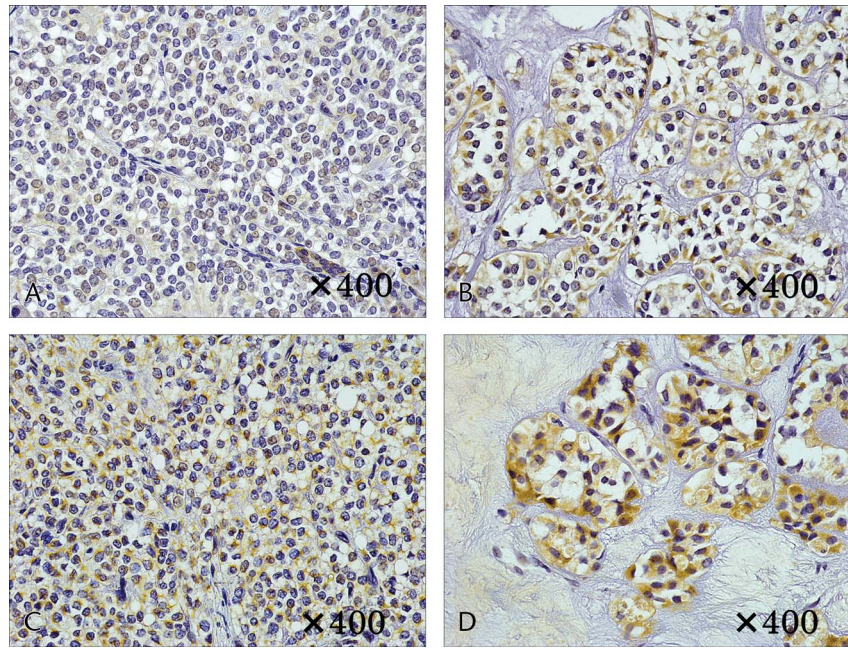

FIGURE 6. Immunostaining of VEGF. A and B, Case 1. A, No cytoplasmic staining in the solid area. B, Weak cytoplasmic staining in the area of necrosis. C and D, Case 6. C, Weak cytoplasmic staining in the solid area. D, Strong cytoplasmic staining in the area of necrosis.

addition, cysts and bleeding are unlikely to occur in SPN with a small tumor diameter, and its differentiation from PDC and PNEN is difficult. Thus, if high FDG uptake is observed in tumors measuring 20 mm or smaller, FDG-PET may be useful for SPN differentiation. Furthermore, in our study, there were no cases with distant metastases or extrapancreatic infiltration, but 9 cases of SPN had vessel invasion or nerve plexus infiltration, with an average SUVmax of 6.2, a value significantly higher than the average of 4.6 for cases with no vessel invasion or nerve plexus infiltration ($P = 0.04$). Solid pseudopapillary neoplasm with high FDG uptake may reflect malignant findings; therefore, FDG-PET may be useful in determining disease stage.

The factors related to FDG uptake in FDG-PET include tumor size, histologic type, and cellular density. The associated

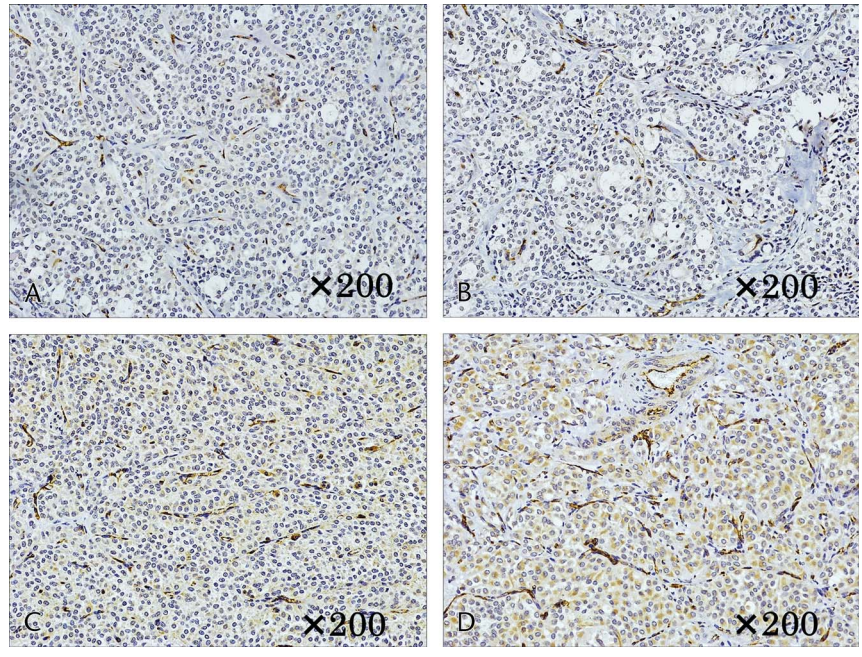

FIGURE 7. Microvessel density measured based on microvessels stained with CD31. A and B, Case 1. Individual vessels were very small in the solid area (A), whereas the area of necrosis had thickening of the vascular walls and crossover of vessels (B). C and D, Case 6. Vessels in the solid area were small (C), whereas the area of necrosis had thickening of the vascular walls and crossover of vessels (D); these changes were more often observed than in case 1.

molecular mechanisms include glucose metabolism and hypoxic environments.[6] The FDG used in FDG-PET is, as with glucose, taken into cells via GLUT-1 that is present in the cell membrane. It is metabolized by hexokinase to form FDG-6-phosphate; however, unlike glucose, it is not further metabolized and remains within the cells. Because there is an increase in glucose metabolism in tumor cells, there is an overexpression of GLUT-1 and an enhanced uptake of FDG. Fluorodeoxyglucose PET uses this principle so that the distribution of FDG within cells can be analyzed.[6,23] The hypoxic environment within tumors is also thought to be connected to FDG uptake. Within cells, a blood circulation imbalance can occur along with increasing tumor size and a hypoxic environment can develop. If the hypoxic environment persists, necrosis will occur in the tissues because of apoptosis; however, in a hypoxic environment, the transcription factor HIF-1 is activated, inducing the glycolytic group of enzymes and increasing glucose uptake into tumor tissue. Neovascularization factors such as VEGF are induced, leading to an increase in new vessels. Uptake of FDG is thought to increase owing to diffusion within the tissue.[19,20,23] Furthermore, a report suggests that HIF-1 is involved in the activation of GLUT-1, and the involvement of molecular mechanisms of GLUT-1, HIF-1, and VEGF with FDG uptake has been reported.[18,19,24]

Higashi et al[14] reported the expression of GLUT in pancreatic tumors, and that although the expression of GLUT1 is not observed in normal pancreatic tissue or inflammatory masses, it is expressed at high levels in various pancreatic tumors including SPN; thus, it is involved in FDG uptake. In addition, Park et al[13] also reported on glucose metabolism in SPN, observing high expression of GLUT1 in SPN. They classified the distributions of FDG uptake within tumors and reported their differences from glucose metabolism activation. Regarding hypoxic environments in pancreatic tumors, Büchler et al[25] reported on the connection between HIF-1 and VEGF in PDC. They observed that once a hypoxic environment was formed, HIF-1 is activated over time, with increased expression of VEGF, changes that were not observed in a normal pancreas. Chen et al[26] reported on the association between HIF-1 and GLUT-1 expression in pancreatic tumors, in which GLUT-1 is controlled by HIF-1 and that inhibition of the HIF-1 enzyme response suppressed the uptake of glucose.

In the present study, GLUT-1, HIF-1, and VEGF were all negatively or weakly expressed in the solid areas of the tumors, whereas slightly higher expression was observed in the necrotic regions. In addition, with increasing tumor diameter, stronger expression was observed in both solid and necrotic areas. One feature of SPN is that its inner characteristics change with increasing tumor diameter. These changes can be observed in typical SPN image findings of cystic degeneration and bleeding. Solid pseudopapillary neoplasm forms as a tumor with high cell density, and a hypoxic environment develops in the center with tumor growth. Hypoxia-inducible factor-1 is activated, resulting in the induction of GLUT-1 (related to glucose metabolism) and VEGF (related to neovascularization). In contrast, necrosis develops in a hypoxic environment and necrotic areas spread with tumor enlargement, resulting in an inflammatory response associated with necrosis and an increased likelihood that bleeding will occur from the increasing vessels.

High cell density is one potential explanation for the high FDG uptake in SPN while the tumor diameter is small; however, although FDG uptake increases with increasing tumor diameter and associated GLUT-1 and VEGF activation, widespread necrotic changes result in lower FDG uptake in necrotic areas and FDG uptake will not increase throughout the entire tumor. Thus, tumors with small diameters have a relatively higher SUVmax than those in PDC and PNEN; however, the increase in SUVmax with increasing tumor diameter may be suppressed.

CONCLUSIONS

When tumor diameter in SPN is small, there are usually no cysts or bleeding; therefore, it is difficult to differentiate it from PDC and PNEN. In the diagnosis of SPN, it is difficult to differentiate from PDC and PNEN with FDG-PET alone; however, it is common for SPN with small tumor diameters to have high SUVmax values compared with those for PDC and PNEN. Therefore, if high FDG uptake is observed in tumors with a small diameter, FDG-PET is potentially useful for the differential diagnosis of SPN. In addition, although cell density and the molecular mechanisms of GLUT-1, HIF-1, and VEGF may be involved in FDG uptake in SPN, the internal characteristics of SPN can significantly change with increased tumor diameter; thus, internal necrotic changes, in particular, have a significant effect on FDG uptake.

REFERENCES

1. Papavramidis T, Papavramidis S. Solid pseudopapillary tumors of the pancreas: review of 718 patients reported in English literature. *J Am Coll Surg*. 2005;2:965–972.
2. Hanada K, Kurihara K, Itoi T, et al. Clinical and pathological features of solid pseudopapillary neoplasms of the pancreas: a nationwide multicenter study in Japan. *Pancreas*. 2018;47:1019–1026.
3. Kang CM, Choi SH, Kim SC, et al. Predicting recurrence of pancreatic solid pseudopapillary tumors after surgical resection: a multicenter analysis in Korea. *Ann Surg*. 2014;260:348–355.
4. Estrella JS, Li L, Rashid A, et al. Solid pseudopapillary neoplasm of the pancreas: clinicopathologic and survival analyses of 64 cases from a single institution. *Am J Surg Pathol*. 2014;38:147–157.
5. Wang X, Chen YH, Tan CL, et al. Enucleation of pancreatic solid pseudopapillary neoplasm: short-term and long-term outcomes from a 7-year large single-center experience. *Eur J Surg Oncol*. 2018;44:644–650.
6. Higashi T, Saga T, Nakamoto Y, et al. Diagnosis of pancreatic cancer using fluorine-18 fluorodeoxyglucose positron emission tomography (FDG PET)—usefulness and limitations in "clinical reality". *Ann Nucl Med*. 2003;17:261–279.
7. Sato M, Takasaka I, Okumura T, et al. High F-18 fluorodeoxyglucose accumulation in solid pseudopapillary tumors of the pancreas. *Ann Nucl Med*. 2006;20:431–436.
8. Shimada K, Nakamoto Y, Isoda H, et al. F-18 fluorodeoxyglucose uptake in solid pseudopapillary tumor of the pancreas mimicking malignancy. *Clin Nucl Med*. 2008;33:766–768.
9. Guan ZW, Xu BX, Wang RM, et al. Hyperaccumulation of (18)F-FDG in order to differentiate solid pseudopapillary tumors from adenocarcinomas and from neuroendocrine pancreatic tumors and review of the literature. *Hell J Nucl Med*. 2013;16:97–102.
10. Dong A, Wang Y, Dong H, et al. FDG PET/CT findings of solid pseudopapillary tumor of the pancreas with CT and MRI correlation. *Clin Nucl Med*. 2013;38:e118–e124.
11. Kim YI, Kim SK, Paeng JC, et al. Comparison of F-18-FDG PET/CT findings between pancreatic solid pseudopapillary tumor and pancreatic ductal adenocarcinoma. *Eur J Radiol*. 2014;83:231–235.
12. Li DL, Li HS, Xu YK, et al. Solid pseudopapillary tumor of the pancreas: clinical features and imaging findings. *Clin Imaging*. 2018;48:113–121.
13. Park M, Hwang HK, Yun M, et al. Metabolic characteristics of solid pseudopapillary neoplasms of the pancreas: their relationships with high intensity ^{18}F-FDG PET images. *Oncotarget*. 2018;9:12009–12019.

14. Higashi T, Tamaki N, Honda T, et al. Expression of glucose transporters in human pancreatic tumors compared with increased FDG accumulation in PET study. *J Nucl Med*. 1997;38:1337–1344.

15. Higashi T, Tamaki N, Torizuka T, et al. FDG uptake, GLUT-1 glucose transporter and cellularity in human pancreatic tumors. *J Nucl Med*. 1998; 39:1727–1735.

16. Kuwai T, Kitadai Y, Tanaka S, et al. Expression of hypoxia-inducible factor-1alpha is associated with tumor vascularization in human colorectal carcinoma. *Int J Cancer*. 2003;105:176–181.

17. Kimura S, Kitadai Y, Tanaka S, et al. Expression of hypoxia-inducible factor (HIF)-1alpha is associated with vascular endothelial growth factor expression and tumor angiogenesis in human oesophageal squamous cell carcinoma. *Eur J Cancer*. 2004;40:1904–1912.

18. Kaira K, Okumura T, Ohde Y, et al. Correlation between 18F-FDG uptake on PET and molecular biology in metastatic pulmonary tumors. *J Nucl Med*. 2011;52:705–711.

19. Toba H, Kondo K, Sadohara Y, et al. 18F-fluorodeoxyglucose positron emission tomography/computed tomography and the relationship between fluorodeoxyglucose uptake and the expression of hypoxia-inducible factor-1α in thymic transporter-1 and vascular endothelial growth factor in thymic epithelial tumors. *Eur J Cardiothorac Surg*. 2013;44: e105–e112.

20. Lin YC, Chen RY, Chen SW, et al. Immunohistochemical studies and fluorodeoxyglucose uptake on positron emission tomography in pharyngeal cancer for predicting radiotherapy-based treatment outcomes. *Clin Otolaryngol*. 2017;42:608–619.

21. Nakagohri T, Kinoshita T, Konishi M, et al. Surgical outcome of solid pseudopapillary tumor of the pancreas. *J Hepatobiliary Pancreat Surg*. 2008;15:318–321.

22. Kang CM, Kim KS, Choi JS, et al. Solid pseudopapillary tumor of the pancreas suggesting malignant potential. *Pancreas*. 2006;32:276–280.

23. Pauwels EK, Strum EJ, Bombardieri E, et al. Positron-emission tomography with [18F] fluorodeoxyglucose. Part I. Biological uptake mechanism and its implication for clinical studies. *J Cancer Ress Clin Oncol*. 2000;126:549–559.

24. Chen C, Pore N, Behrooz A, et al. Regulation of glut1 mRNA by hypoxia-inducible factor-1. Interaction between H-ras and hypoxia. *J Biol Chem*. 2001;276:9519–9525.

25. Büchler P, Reber HA, Büchler M, et al. Hypoxia-inducible factor 1 regulates vascular endothelial growth factor expression in human pancreatic cancer. *Pancreas*. 2003;26:56–64.

26. Chen J, Zhao S, Nakada K, et al. Dominant-negative hypoxia-inducible factor-1 alpha reduces tumorigenicity of pancreatic cancer cells through the suppression of glucose metabolism. *Am J Pathol*. 2003;162:1283–1291.